Topics in Catalysis (2022) 65:1225–1234
https://doi.org/10.1007/s11244-022-01624-3

ORIGINAL PAPER

17 α-Ethinylestradiol Degradation in Continuous Process by Photocatalysis Using Ag/Nb_2O_5 Immobilized in Biopolymer as Catalyst

Giane G. Lenzi[1] · Eduardo Abreu[1,2] · Maria Eduarda K. Fuziki[2] · Michel Z. Fidelis[2] · Rodrigo Brackmann[3] · Jose L. Diaz de Tuesta[4] · Helder T. Gomes[4] · Onélia A. A. dos Santos[2]

Accepted: 22 April 2022 / Published online: 23 May 2022

Abstract
This study describes the application of Ag/Nb_2O_5 catalysts, suspension and spheres alginate immobilized for the degradation of 17α-Ethinylestradiol (EE2). The techniques used to characterize the photocatalysts were as follows: X-ray diffraction (XRD), N_2 adsorption–desorption analysis (BET), point charge zero charge (PZC), scanning electron microscopy (SEM) and energy dispersive X-ray spectroscopy (EDS)**.** Different catalyst calcination temperatures were studied by keeping the silver metal loading at 5%. Among the operational conditions analyzed were pH, catalyst concentration, the emitting source of radiation and the inlet flow rate (in continuous operation). The results of the experiments performed initially with the catalyst in suspension revealed that the highest catalytic activity in the degradation of EE2 was the $5\%Ag/Nb_2O_5$ catalyst calcined at 973 K, which removed 77.7% of the initial pollutant concentration in 120 min of reaction. The immobilization of the catalyst in alginate spheres resulted in a degradation reduction, being able to degrade 69.2% of the initial EE2 in a batch system. In the continuous system, the immobilized catalyst obtained a total degraded of 37.3%, with a flow rate of 10 $L{\cdot}h^{-1}$. Catalyst reuse was promising, even dropping the removal, degrading around 27% of the initial EE2 concentration in the third cycle of use.

Keywords Spheres alginate · Emerging pollutants · Contaminants of emerging concern · Advanced oxidation process · Thermal treatment

1 Introduction

The increasing use of chemical compounds combined with the low efficiency of collection and treatment of domestic and industrial effluents, has led to a significant increase in emerging contaminants found in surface waters. Because of this, part of the scientific community turns its research to the analysis of the quality of water bodies. With the advancement of more precise techniques and methods, it is possible to identify and quantify more compounds and substances present in water [1]. These chemical species are called emerging contaminants, some of them are: drugs, endocrine disruptors and personal care products [2]. Among these substances, some of the most harmful are endocrine disruptors, such as 17α-ethinylestradiol (EE2), which is used in hormone replacement therapy during menopause, the treatment of some hormonal disorders and as a contraceptive [3]. However, EE2 is extremely toxic to aquatic ecosystems, causing feminization in fish [4] and increasing the incidence

✉ Giane G. Lenzi
gianeg@utfpr.edu.br

1 Departamento de Engenharia Química, Universidade Tecnológica Federal do Paraná, Rua Doutor Washington Subtil Chueire, 330, Ponta Grossa, PR 84017-220, Brazil

2 Departamento de Engenharia Química, Universidade Estadual de Maringá, Avenida Colombo, 5790, Maringá, PR 87020-900, Brazil

3 Departamento de Química, Universidade Tecnológica Federal do Paraná, Via do Conhecimento, s/n—Km 01, Pato Branco, PR 85503-390, Brazil

4 Centro de Investigação de Montanha (CIMO), Instituto Politécnico de Bragança, Campus de Santa Apolónia, 5300-253 Bragança, Portugal

of certain types of cancer and endometriosis in humans [5]. Heterogeneous photocatalysis is of great interest due to its applicability and high potential as a method of pollutant degradation, being able to mineralize such compounds and transform them into carbon dioxide, water and inorganic anions. This process is characterized by the activation of a semiconductor, such as TiO_2, ZnO, ZrO_2, Cu_2O, SnO_2, CdS by solar or artificial radiation [6, 7]. Among the photocatalysts, TiO_2 is the most used due to its low cost, non-toxicity, and high chemical stability. Nb_2O_5-based catalysts are a promising alternative that has emerged in a relatively short time, due to the niobium pentoxide similarities with TiO_2, in addition to its chemical stability and atoxicity [8]. There are few researches carried out on the application of Nb_2O_5 as a photocatalyst, when compared to studies involving TiO_2. Some studies, such as those conducted by Josué et al. [9], applied Nb_2O_5 in the reduction of Cr (VI) and obtained a 20% better result using Nb_2O_5 when compared to TiO_2. Fidelis et al. [6], applied Fe/Nb_2O_5 catalyst immobilized in the degradation of triclosan, achieving promising results. In this context, the present work was carried out using an Ag-promoted Nb_2O_5-based catalyst for the photocatalytic process in the degradation of the hormone 17α-ethinylestradiol in water. A design of experiment (DoE) was applied to investigate the optimal operating conditions for the batch system and then was extended to the continuous system using the catalyst immobilized on alginate spheres.

2 Experimental Procedure

2.1 Chemicals

The reagents used in this study were: 17α-Ethinylestradiol (Merck, Germany), Nb_2O_5, supplied by Companhia Brasileira de Metalurgia e Mineração (CBMM), Silver Nitrate P.A. A.C.S. (Synth, Brazil), as precursor, absolute ethyl alcohol P.A. A.C.S. 99.5% (Synth, Brazil). Acetonitrile for HPLC (Merck, Germany). Sodium alginate P.A. (Sigma Aldrich, USA) and calcium chloride P.A. (Nuclear, Brazil) for the immobilization process. Sodium hydroxide (Neon, Brazil) and hydrochloric acid (Química Moderna, Brazil) for pH control.

2.2 Analytical Control

During the experiments, the technique used to quantify EE2 was based on the methodology employed by Moon and Myung [10], using high performance liquid chromatography (HPLC). The authors used the method aiming to determine estrogens in environmental aqueous samples, witch ones were previously been microextracted using dispersive liquid–liquid microextraction technique. In this research we used the conditions from the chromatographic separation and quantitative analysis they employed. A chromatograph (YL Clarity 9100) equipped with pre-column, C-18 column (Phenomenex) and visible ultraviolet detector (UV–Vis) was used. The measured wavelength was 225 nm and EE2 elution occurred within 5 min. The mobile phase is composed of acetonitrile and ultrapure water, in a proportion of 45:55, respectively, with an injection of 20 µL of sample.

2.3 Preparation of Ag/Nb_2O_5 Catalysts

The Ag/Nb_2O_5 catalysts were synthesized by excess solvent impregnation with nominal loading of 5 wt.% Ag and subsequently calcined at different temperatures (373, 473, 573, 673, 773, 873 and 973 K). The catalyst with the highest photocatalytic activity was immobilized in calcium alginate beads, from sodium alginate solution (2% w/v) and the catalyst selected (2% w/v) in ultrapure water. This solution was dripped using a peristaltic pump onto a calcium chloride solution (2% w/v) at 278 K. The spheres were kept refrigerated in a $CaCl_2$ solution for 24 h, washed and then dried in an oven for 8 h at 333 K. The catalysts were characterized by different techniques, namely N_2 adsorption/desorption, Point of Zero Charge (PZC), X-ray diffraction (XRD) and scanning electron microscopy (SEM) and energy-dispersive X-ray spectroscopy (EDS).

2.4 Catalysts Characterization

2.4.1 Point of Zero Charge (PZC)

The point zero charge (PZC) determination was performed by applying the methodology described by Regalbuto and Robles [15]. In 125 mL Erlenmyer flasks, 50 mg of catalyst and 50 mL of ultrapure water were mixed, under different initial pH values (2, 3, 4, 5, 6, 7, 8, 9, 10, 11 and 12). After constant stirring for 24 h in a shaker at 298 K and 120 rpm, the final pH measurements of the suspensions were performed. The pHPZC corresponded to the average of the final pH values which tended to a constant value, regardless of the initial pH value.

2.4.2 Scanning Electron Microscopy (SEM) and Energy-Dispersive X-Ray Spectroscopy (EDS)

The scanning electron microscopy (SEM) and energy-dispersive X-ray spectroscopy (EDS) analysis were performed in a Tescan Scanning Electron Microscope, Vega 3 LMU equipped with dispersive energy detector –EDS- Oxford, AZTec Energy X-Act.

2.4.3 X-Ray Diffraction

The samples were analyzed in a Rigaku-Denki Diffractometer with aCu-Kα radiation (λ = 1.5406 Å) at a voltage of 140 V and current of 40 mA. Thus, the obtained patterns were compared with the diffraction dataset cards from the International Center for Diffraction Data (ICDD)0.2.3.3.

2.5 Photocatalytic Tests

In order to find the most suitable calcination temperature were carried out a series of test in a batch system. These tests consisted of 30 min of dark adsorption, followed by 120 min of photocatalysis. The batch system used in the experiments is shown in Fig. 1a, containing a 125 W mercury vapor lamp (without the protective bulb), a 250 mL borosilicate jacketed reactor, a magnetic stirrer and an atmospheric air pump, in addition to a thermostatic bath, to maintain the temperature at 293 K.

These tests were carried out with a catalyst concentration of 1 $g{\cdot}L^{-1}$. A face-centered central composite design was performed, considering two factors: pH values and catalyst concentration, which were evaluated for immobilized catalyst (Table 2). Tests were also performed in the continuous system (Fig. 1b), considering the experimental conditions with the best EE2 degradation results obtained in the batch system**.** The prototype was equipped with 10 tubular borosilicate reactors. Stainless steel filters were placed at the inlets and outlets of the tubes. Two radiation sources were used in the continuous system: (1) mercury lamps of 125 W (without the protective bulb), and (2) black light lamps of 25 W each. All experiments were conducting using a 10 $mg{\cdot}L^{-1}$ synthetic EE2 solution.

For continuous tests, the immobilized catalyst was placed between the filters, separated by 20 cm, in 5 of the 10 reactors, operating under ideal conditions. Three different flows were selected, namely 10, 20 and 40 $L{\cdot}h^{-1}$. The hydraulic residence time for these flows were 22, 11 and 5.5 min, respectively. In each continuous test, the time to reach steady state was 44 min (10 $L{\cdot}h^{-1}$), 22 min (20 $L{\cdot}h^{-1}$) and 11 min (40 $L{\cdot}h^{-1}$). These tests were performed in triplicate.

For the photolytic tests, the same procedures were carried out, however, without the presence of the catalyst.

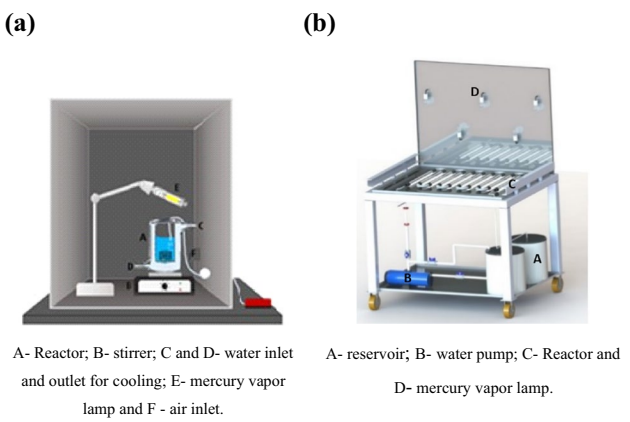

Fig. 1 **a** Batch system scheme; **b** Continuous process prototype

3 Results and Discussion

3.1 Adsorption, Photolysis and Photocatalytic Tests

3.1.1 Powder Catalysts

The results of adsorption, photolysis and photocatalysis processes in the degradation of 17α- ethinylestradiol (EE2) for different catalyst calcination temperatures are shown in Fig. 2a and b. As observed, even the catalysts calcined at 773 K and 873 K which showed the lowest catalytic activities (with a reaction rate constant of 0.0081 and 0.0050 min^{-1} respectively), exhibited better results than photolysis, indicating the influence of Ag-promoted semiconductor for the degradation of EE2. Almeida et al. [11] used ZnO and TiO_2 with 5% silver and obtained high caffeine degradation under optimized conditions and using a 125 W mercury. Chaker et al. [12] employed Ag in TiO_2 in a photocatalytic reaction in order to disinfect water containing *E. coli*, the authors described that Mesoporous TiO_2 materials modified with Ag displayed significant capacities for the degradation of MO and wastewater under UV and simulated solar light irradiation compared with P25 TiO_2. The enhanced photocatalytic activity of Ag/TiO_2 can be ascribed to a strong inhibition of $e^- - h^+$ recombination. 0.5 wt.% Ag/TiO_2 exhibited the highest TOC abatement for both MO and wastewater effluent. Lenzi et al. [13] reduced Hg^{2+} em photocatalytic process using an Ag/TiO_2 catalyst. The result indicated that the photocatalytic activity indicated that the reduction ratio of Hg^{2+} to Hg^0 was influenced by the photocatalyst synthetic method, calcination temperature, and Ag addition.

The 5% Ag / Nb_2O_5 catalysts calcined at 973 K presented the highest EE2 removal (~ 78%, k = 0.0128 min^{-1}), when compared to the other catalysts studied. Paulis et al. [14] studied the effects of calcination temperature of Nb_2O_5 on its catalytic activity for aldol condensation of acetone. It was observed that the increase in the calcination temperature caused a decrease in the specific surface area. Despite this, the specific activity increases gradually, except for the sample calcined at 1173 K. Changes in the crystalline phase were observed in samples calcined at 673, 773, 973 and 1173 K. When heated to 773 K, Nb_2O_5 presents the hexagonal system. At 973 K the splitting of the peaks is observed and the new crystalline system is in agreement

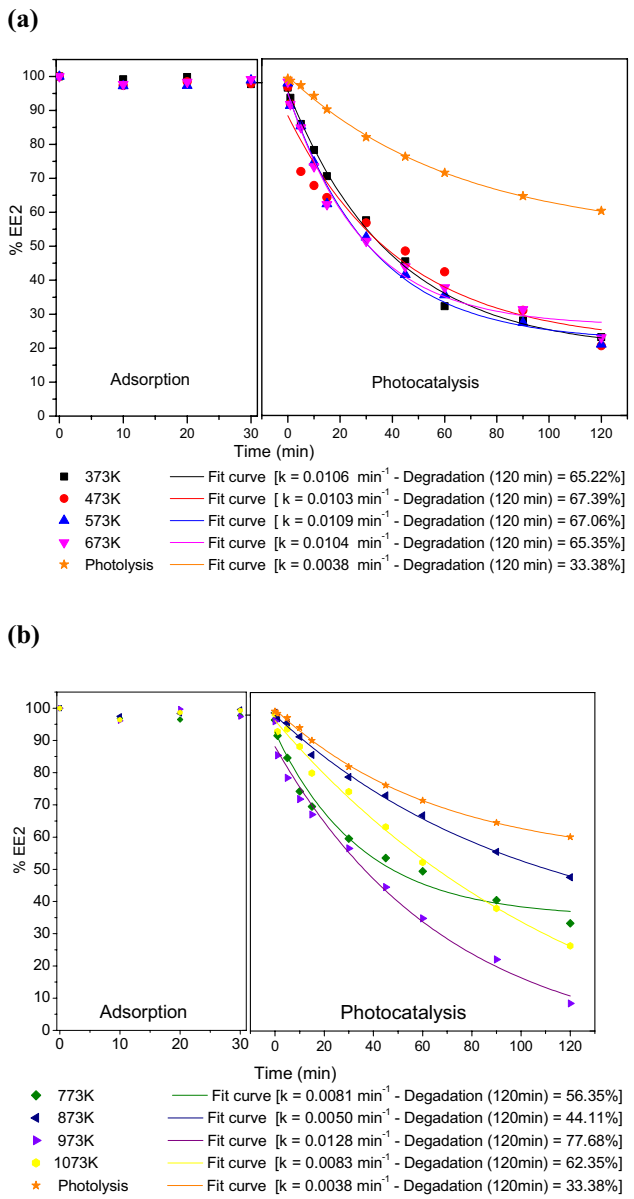

Fig. 2 Initial tests with 5%Ag/Nb_2O_5 catalysts under different calcination temperatures: (**a**) and (**b**)

with the orthorhombic phase and the sample calcined at 1173 K crystallizes in the monoclinic system.

Thus, the catalyst calcined at 973 K was selected for the immobilization process in biopolymer (alginate spheres/beads). The characterizations of the catalyst calcined at 973 K indicated: Specific surface area (BET) of 4 $m^2 \cdot g^{-1}$ and pore volume equal to 0.04 m^3·g-1 (Table 1).

Some authors indicate that calcination temperature increasing and metal addition to the catalyst may lead to a reduction in the specific surface area. This is due to sintering and blocking pores by metal [15], respectively.

Table 1 Specific surface area (S_o) and microporevolume (Vm)

Catalyst 5%Ag/Nb_2O_5	S_o (m^2 g^{-1})	Vm (cm^3 g^{-1})
Calcined at 973 K	4	0.040
Spheres non-calcined	36	0.036
Spheres calcined at 973 K	6	0.022

Point of zero charge (PZC), analysis indicated a value of 6.70 for 5% Ag/Nb_2O_5 calcined at 973 K, Fig. 3a. The values present in the literature for pure niobium, however, are lower, in a range from 3.90 to 4.94. In the work developed by Domingues et al. (2019), Nb_2O_5 was used to degrade textile effluent dye, and the value found for PCZ was 3.90 [16]. Kosmulski (2009) described the value of 4.10 [17], while Bolzon and Prado (2011) 4.94 [18]. Santos et al. used niobium pentoxide to discoloration textile effluent containing azodyes obtained a PZC value of 4.86. Scanning electron microscopy (SEM/EDS) images (Fig. 3b and c), indicated a rough and porous catalytic surface, with uniformly dispersed Ag distribution. X-ray diffraction (XRD) results for 5% Ag/Nb_2O_5 catalyst calcined at 973 K indicated the presence of $AgNb_7O_{18}$ (PDF# 21-1084) and $AgNb_{13}O_{33}$ (PDF# 21-1083) in the sample, as it can be observed in Fig. 4. These phases can only be obtained from Ag and Nb_2O_5 precursors calcined at elevated temperatures. Considering pure niobium pentoxide, Fidelis et al. [19] observed that non-calcined Nb_2O_5 samples, initially with amorphous structure, transformed into TT and T-Nb_2O_5 crystalline phases when calcined at temperatures higher than 673 K (773–873 K). Liu et al. and Chen et al., could only obtain the $AgNb_{13}O_{33}$ phase after calcining their samples, respectively, at 1073 K for 3 h [20] and 1263 K for 12 h [21]. According to the authors, the material presents a typical perovskite-like structure, a triclinic lattice with space group C1 (1) [21]. Liu et al. also highlighted its potential as a photocatalyst for the degradation of organic pollutants [20]. Similarly, $AgNb_7O_{18}$ can be produced at high calcination temperatures, between 1073 K [22] and 1523 K [23], as reported in the literature. This phase has a orthorhombic structure (space group Immm(71)) and presents photocatalytic activity, having already been tested in the degradation of methylene blue [22].

The Rietveld refined (Fig. 5) performed based on the works of [20–23], presented a reasonable fit ($\chi^2 = 5.752$), and indicated a sample composition of 65.6% de $AgNb7O_{18}$ e 34.4% de $AgNb_{13}O_{33}$.

3.1.2 Immobilized Catalyst

The adsorption test result for the 5% Ag/Nb_2O_5 catalyst calcined at 973 K and immobilized in the biopolymer (alginate) beads is shown in Fig. 6a. Furthermore, the characterizations

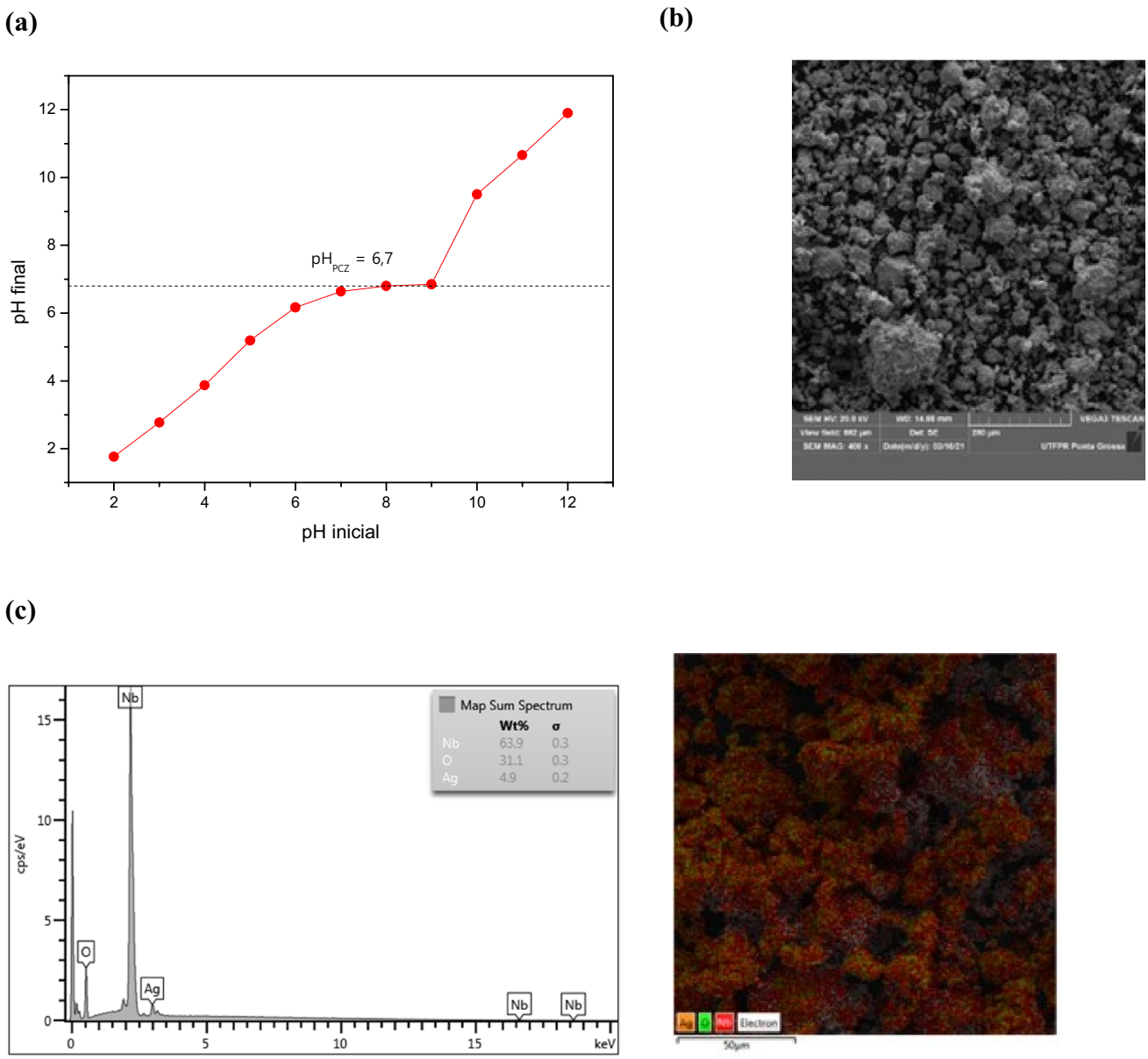

Fig. 3 Characterization results of 5% Ag/Nb_2O_5 catalyst calcined at 973 K: **a** PZC; **b** SEM and **c** EDS

of this catalyst after immobilization are shown in Fig. 7a, b and c.

It is observed that the adsorption–desorption process occurs simultaneously Fig. 6. This result indicates that adsorption is not the predominant phenomenon for the removal of EE2 from the medium. This result is in agreement with that described in the literature. Zhang et al. [24] studied the adsoption effect on Ag-modified helical chiral TiO_2 NFs. Observed a decrease of 3–5% in EE2 concentration within 30 min, indicating the little adsorption of EE2. Li et al. [25] monitored the degree of EE2 adsorption onto the (TiO2) catalyst surface in the dark the result indicated only 3% of its initial concentration.

The characterizations of the immobilized 5%Ag/Nb_2O_5 catalyst calcined at 973 K indicated: Specific surface area (BET) of 6 $m^2 \cdot g^{-1}$ for the 5%Ag/Nb_2O_5 catalyst calcined to 973 K and immobilized in alginate spheres (Table 1). On the other hand, when compared to pure non-calcined niobium pentoxide immobilized, we observed a greater surface area of 36 $m^2 \cdot g^{-1}$. This is due to the calcination process and addition of the promoter to the catalyst. The X-ray diffraction analysis indicated that the catalyst immobilization in alginate spheres did not change the crystal structure of the materials. The diffractograms revealed the amorphous structure of non-calcined Nb_2O_5 immobilized catalyst (Fig. 7a).

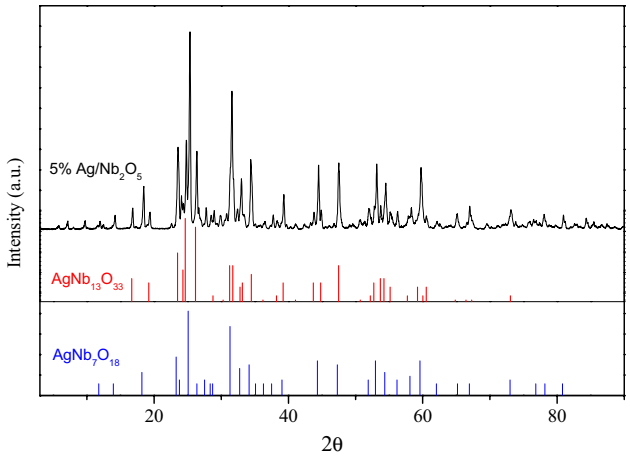

Fig. 4 Diffractogram of 5%Ag/Nb_2O_5 catalysts calcined at 973 K in comparison to the standard peaks of phases $AgNb_7O_{18}$ (PDF# 21-1084) and $AgNb_{13}O_{33}$ (PDF# 21-1083)

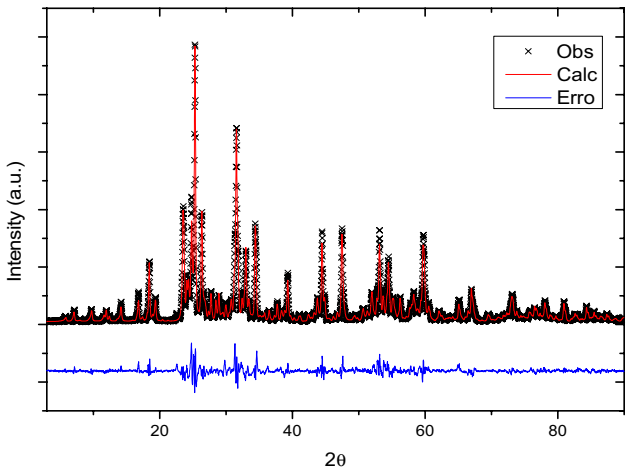

Fig. 5 Rietveld refinement result

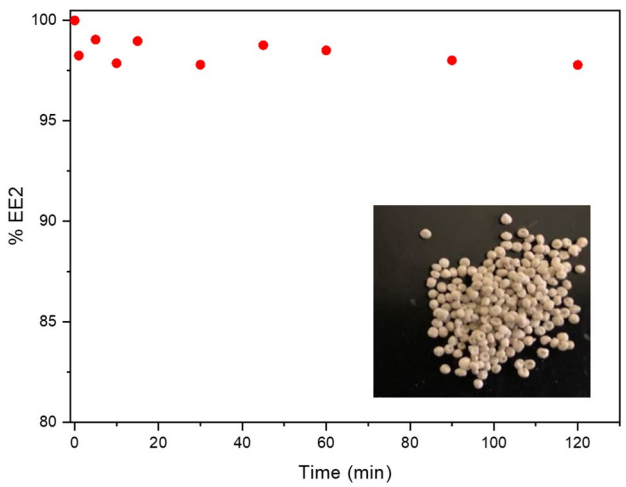

Fig. 6 Adsorption process 5%Ag/Nb_2O_5 immobilized in biopolymer

The results obtained for PCZ of the catalysts are shown in Fig. 7b. It was observed that for the non-calcined sample Nb_2O_5 and 5% Nb_2O_5 calcined at 973 K of alginate spheres, there are no significant changes in PCZ around 5.66. The obtained SEM image indicated that the 5% Ag/Nb_2O_5 photocatalysts (Fig. 7c) presented a surface lumpy and the estimated elementary surface composition, given by the EDS analysis, demonstrated the presence Ag in the surface.

As it can be seen in Table 2, the highest EE2% degradation results were obtained in the lowest pH tested (pH = 4 and catalyst concentration 1.5 g L^{-1}). According to the data and the level curve (contour plot Fig. 8), in this experimental design tests, neutral pH was the one which removed the least pollutant from the medium, between 50 and 55%, results may be related to the proximity of the catalyst to the ZPC when operating at pH 7. For the case of immobilized catalyst, the best conditions were pH 4 and 1.5 g·L^{-1}, removing 69% of the initial EE2. The Anova Table was generated with $R^2 = 0.9892$.

The best conditions were used in the continuous process (pH = 4, 5%Ag/Nb_2O_5 immobilized catalyst calcined at 973 K).

3.2 Continuous Process

The results from the tests in continuous process are shown in the Figs. 9 and 10.

The degradation of EE2 for tests with radiation provided by the mercury vapor lamp was greater when compared to tests with black light radiation (Fig. 9). In theory, glass absorbs more significantly the UV radiation emitted by the black light lamp, causing a smaller amount of radiation to actively reach the catalyst. With the increase in flow, the time of exposure to radiation decreases, resulting in less pollutant removal. For the best case, the photocatalysis with the Hg vapor lamp, the removals percentages obtained were 37.3; 28.1 and 16.8% for the flows of 10, 20 and 40 L·h^{-1}, respectively. Comparing the results of photolysis *vs* photocatalysis, the use of the catalyst proved to be a necessary to increase the hormone removal efficiency. In the use of black light, the application of the immobilized catalyst represented an increase of one percentage unit in total degradation, operating at a flow rate of 10 L·h^{-1}, with a jump from 5.4 to 6.6%. As for the mercury vapor lamp, degradation jumped from 27.7 to 37.7%, an increase of 10 percentage units. The analysis of these data reinforces the importance of applying the photocatalysts in the pollutant removal process.

Catalyst reuse tests were carried out in the continuous system, with the 2 radiation sources. The flow rate of 10 L·h^{-1} was used to evaluate reuse. These results are shows in the Fig. 10.

Cycle 1 refers to the first use of the catalyst, cycle 2 to the first reuse and the cycle 3 to the second reuse. Degradation

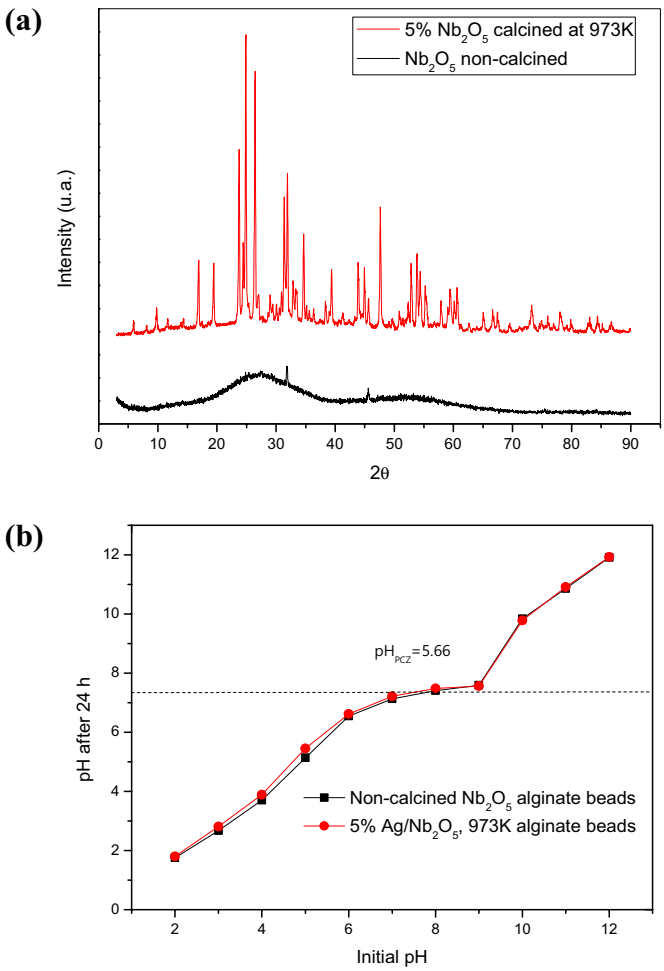

Fig. 7 Characterization results **a** XRD; **b** PZC; and **c** SEM/EDS, immobilized catalyst

Table2 Experimental design matrix and experimental response (5%Ag/Nb_2O_5 calcined at 973 K and immobilized in calcium alginate beads)

Run	pH	Catalyst Concentration (g L^{-1})	% Degradation	k (min^{-1})	R^2
1	4 (−1)	0.5 (−1)	64.7	0.0093	0.9824
2	4 (−1)	1.0 (0)	67.8	0.0100	0.9899
3	4 (−1)	1.5 (+1)	69.2	0.0106	0.9880
4	7 (0)	0.5 (−1)	50.3	0.0066	0.9801
5	7 (0)	1.0 (0)	53.8	0.0069	0.9753
6	7 (0)	1.5 (+1)	55.7	0.0071	0.9831
7	10 (+1)	0.5 (−1)	56.9	0.0073	0.9886
8	10 (+1)	1.0 (0)	56.6	0.0074	0.9922
9	10 (+1)	1.5 (+1)	58.0	0.0073	0.9923

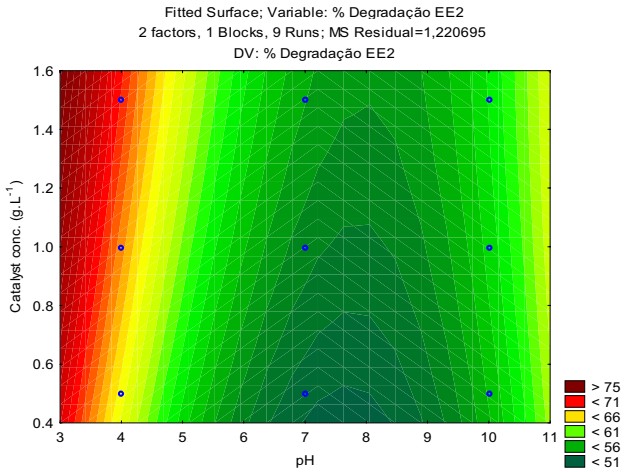

Fig. 8 Fitted surface for 5%Ag/Nb_2O_5 immobilized catalyst

was much less effective when using black light as a source of radiation, but the degradation was not very expressive, compared with the other results obtained. Analyzing the catalyst reuse applying the Hg vapor lamp, the reduction in removal is more relevant between cycle 1 and 2, than between cycle

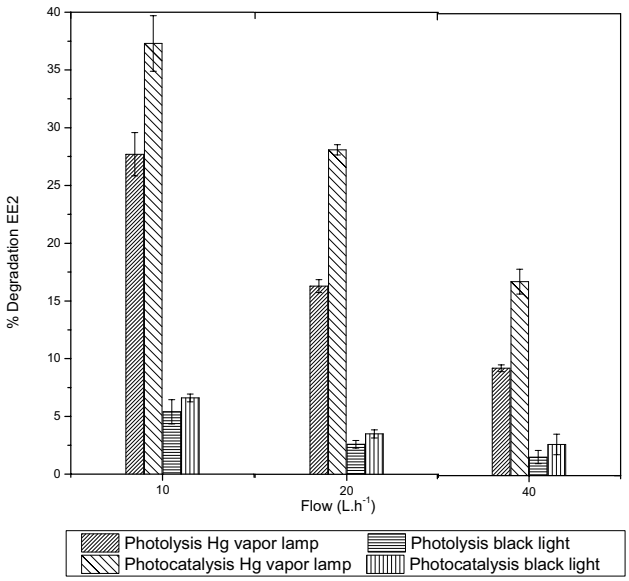

Fig. 9 Degradation of EE2 under different inlet flow rates

2 and 3. The removal percentages were 35.5; 26.8 and 24.3% for cycles 1, 2 and 3 respectively.

4 Conclusions

Heterogeneous photocatalysis process using Ag/Nb_2O_5 catalysts is efficient for the degradation of EE2, indicating that it is a viable alternative. For continuous process application, the radiation emitted by the black light lamp was less efficient when compared to the mercury vapor lamp (photolysis). The difference is greater when the degradation values via photocatalysis are pointed out, in which the use of black light removed 6.6%, opposing at 37.3% of the degradation achieved by the radiation emitted by the Hg vapor lamp. Catalyst reuse led to a drop of 11.2 percentage points in 3 cycles of use (35.5% in the 1st to 24.3% in the 3rd), pointing out that the recovery and reactivation process can be improved, aiming to reduce loss of performance.

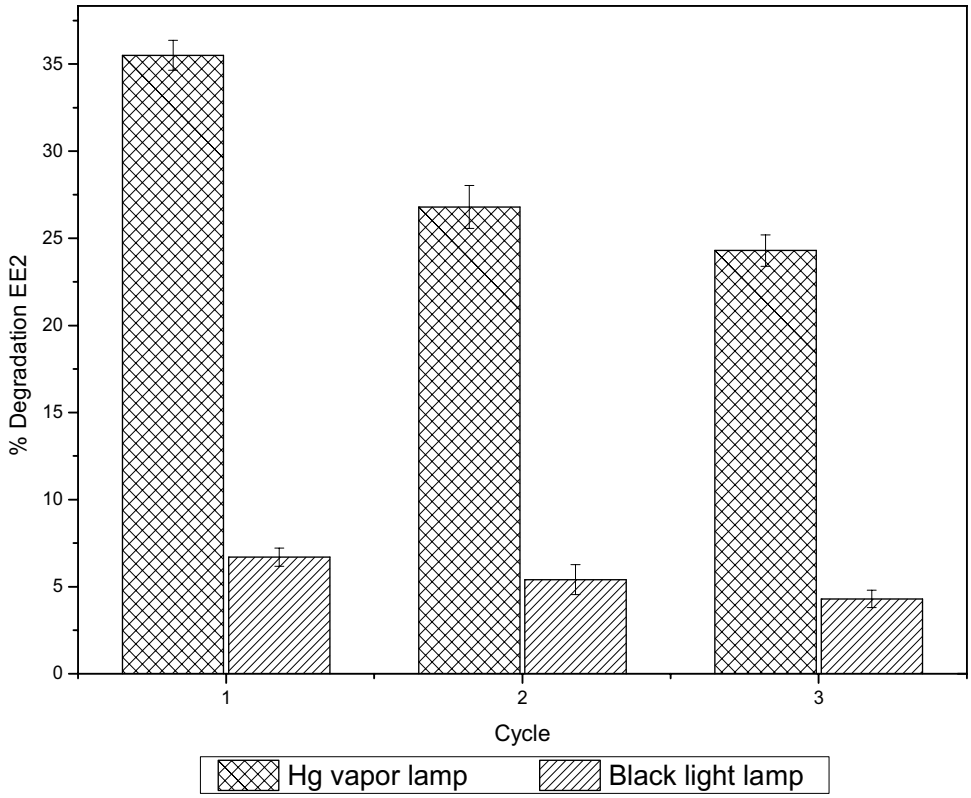

Fig. 10 Reuse of the catalyst (up to three cycles) for the degradation of EE2 under Hg vapor and black light lamps

Acknowledgements The authors are thankful to the Brazilian agencies CNPq, CAPES and Fundação Araucária for financial support of this work, C^2MMa and Brazilian Mining and Metallurgy Company – CBMM and are grateful to the Foundation for Science and Technology (FCT, Portugal) and FEDER (Fundo Eropeu de Desenvolvimento Regional) under Programme PT2020 for financial support to CIMO (UIDB/00690/2020).

References

1. Cates EL (2017) Photocatalytic water treatment: so where are we going with this? Environ Sci Technol 51:757–758. https://doi.org/10.1021/acs.est.6b06035
2. Focazio MJ, Kolpin DW, Barnes KK et al (2008) A national reconnaissance for pharmaceuticals and other organic wastewater contaminants in the United States - II) Untreated drinking water sources. Sci Total Environ 402:201–216. https://doi.org/10.1016/j.scitotenv.2008.02.021
3. Ribeiro CCM, Shimo AKK, de Lopes MHB, Lamas JLT (2018) Effects of different hormonal contraceptives in women's blood pressure values. Rev Bras Enferm 71:1453–1459. https://doi.org/10.1590/0034-7167-2017-0317
4. da Cunha DL, da Silva SMC, Bila DM et al (2016) Regulation of the synthetic estrogen 17α-ethinylestradiol in water bodies in Europe, the United States, and Brazil. Cad Saude Publica 32:e00056715. https://doi.org/10.1590/0102-311X00056715
5. Froehner S, Souza DB, MacHado KS, Da Rosa EC (2010) Tracking anthropogenic inputs in Barigui River, Brazil using biomarkers. Water Air Soil Pollut 210:33–41. https://doi.org/10.1007/s11270-009-0220-8
6. Fidelis MZ, Abreu E, Josué TG et al (2020) Continuous process applied to degradation of triclosan and 2.8-dichlorodibenzene-p-dioxin. Environ Sci Pollut Res. https://doi.org/10.1007/s11356-020-10902-0
7. Serna-Galvis EA, Botero-Coy AM, Martínez-Pachón D et al (2019) Degradation of seventeen contaminants of emerging concern in municipal wastewater effluents by sonochemical advanced oxidation processes. Water Res 154:349–360. https://doi.org/10.1016/j.watres.2019.01.045
8. Yan J, Wu G, Guan N, Li L (2014) Nb2O5/TiO2 heterojunctions: Synthesis strategy and photocatalytic activity. Appl Catal B Environ 152–153:280–288. https://doi.org/10.1016/j.apcatb.2014.01.049
9. Josué TG, Almeida LNB, Lopes MF et al (2020) Cr (VI) reduction by photocatalyic process: Nb2O5 an alternative catalyst. J Environ Manage 268:110711. https://doi.org/10.1016/j.jenvman.2020.110711
10. Moon YJ, Myung SW (2016) Determination of estrogens in environmental aqueous samples using dispersive liquid-liquid microextraction and HPLC/UV–vis system. Bull Korean Chem Soc 37:2009–2014. https://doi.org/10.1002/bkcs.11016
11. Almeida LNB, Lenzi GG, Pietrobelli JMTA, Santos OAA (2019) Caffeine degradation using ZnO and Ag/ZnO under UV and solar radiation. Desalin Water Treat 153:85–94. https://doi.org/10.5004/dwt.2019.24045
12. Chaker H, Chérif-Aouali L, Khaoulani S et al (2016) Photocatalytic degradation of methyl orange and real wastewater by silver doped mesoporous TiO2 catalysts. J Photochem Photobiol A Chem 318:142–149. https://doi.org/10.1016/j.jphotochem.2015.11.025
13. Lenzi GG, Fávero CVB, Colpini LMS et al (2011) Photocatalytic reduction of Hg(II) on TiO2 and Ag/TiO2 prepared by the sol–gel

and impregnation methods. Desalination 270:241–247. https://doi.org/10.1016/j.desal.2010.11.051
14. Paulis M, Martín M, Soria D et al (1999) Preparation and characterization of niobium oxide for the catalytic aldol condensation of acetone. Appl Catal A Gen 180:411–420. https://doi.org/10.1016/S0926-860X(98)00379-2
15. Gonçalves G, Lenzi MK, Santos OAA, Jorge LMM (2006) Preparation and characterization of nickel based catalysts on silica, alumina and titania obtained by sol–gel method. J Non Cryst Solids 352:3697–3704. https://doi.org/10.1016/j.jnoncrysol.2006.02.120
16. Domingues FS, Geraldino HCL, de Freitas TKF et al (2019) Photocatalytic degradation of real textile wastewater using carbon black-Nb_2O_5 composite catalyst under UV/Vis irradiation. Environ Technol. https://doi.org/10.1080/09593330.2019.1701565
17. Kosmulski M (2009) Surface Charging and Points of Zero Charge. CRC Press, Boca Raton
18. Bolzon LB, Prado AGS (2011) Effect of protonation and deprotonation on surface charge density of Nb_2O_5. J Therm Anal Calorim 106:427–430. https://doi.org/10.1007/s10973-011-1316-0
19. Fidelis MZ, Abreu E, Dos Santos O et al (2019) Experimental design and optimization of triclosan and 2.8-diclorodibenzeno-p-dioxina degradation by the Fe/Nb2O5/UV system. Catalysts 9:343. https://doi.org/10.3390/catal9040343
20. Liu X, Qin C, Huang Y et al (2017) A new silver niobate photocatalyst $AgNb_{13}O_{33}$: synthesis, structure and photochemical properties. J Taiwan Inst Chem Eng 78:530–538. https://doi.org/10.1016/j.jtice.2017.06.034
21. Chen Z, Cheng X, Ye W et al (2019) AgNb13O33: a new anode material with high energy storage performance. Chem Eng J 366:246–253. https://doi.org/10.1016/j.cej.2019.02.091
22. Liu XX, Qin C, Cao L et al (2017) A silver niobate photocatalyst AgNb7O18 with perovskite-like structure. J Alloys Compd 724:381–388. https://doi.org/10.1016/j.jallcom.2017.07.048
23. Woodward DI, Beanland R (2014) ChemInform abstract: AgNb 7 O 18: an ergodic relaxor ferroelectric. ChemInform https://doi.org/10.1002/chin.201442005
24. Zhang C, Li Y, Wang D et al (2015) Ag@helical chiral TiO2 nanofibers for visible light photocatalytic degradation of 17α-ethinylestradiol. Environ Sci Pollut Res 22:10444–10451. https://doi.org/10.1007/s11356-015-4251-y
25. Li S, Sun W (2014) Photocatalytic degradation of 17α-ethinylestradiol in mono- and binary systems of fulvic acid and Fe(III): Application of fluorescence excitation/emission matrixes. Chem Eng J 237:101–108. https://doi.org/10.1016/j.cej.2013.10.002